УДК 556.078:532.517.4

© *С. Ю. Волков*[1], *С. Р. Богданов*[1,2], *Г. Э. Здоровеннова*[1]*, *А. Ю. Тержевик*[1], *Р. Э. Здоровеннов*[1], *Н. И. Пальшин*[1], *Т. В. Ефремова*[1], *Г. Б. Кириллин*[3]

[1]Институт водных проблем севера Карельского научного центра РАН, 185030, пр. Александра Невского, д. 50, г. Петрозаводск, Республика Карелия, Россия
[2]Петрозаводский государственный университет, 185910, пр. Ленина, 33, г. Петрозаводск, Республика Карелия, Россия
[3]Лейбниц-Институт пресноводной экологии и рыболовства во внутренних водоемах (IGB), г. Берлин, Германия (Мюггельзедамм 310, 12587)
*E-mail: zdorovennova@gmail.com

МЕТОД ОЦЕНКИ ПАРАМЕТРОВ АНИЗОТРОПИИ МЕЛКОМАСШТАБНОЙ ТУРБУЛЕНТНОСТИ ПО ДАННЫМ АКУСТИЧЕСКИХ ПРОФИЛОГРАФОВ

Статья поступила в редакцию 09.10.2020, после доработки 23.12.2020

Акустические допплеровские профилографы течений широко используются для построения вертикальных профилей скорости. В последние годы эти приборы применяются также для оценок скорости ε диссипации энергии, на основе анализа продольных структурных функций. Применимость этих оценок, однако, остается спорной, поскольку расчет осуществляется в рамках предположения о локальной однородности и изотропности мелкомасштабных пульсаций и с использованием канонических значений констант Колмогорова. Однако во многих случаях, как показывают экспериментальные исследования и прямые численные расчеты, эти константы существенно варьируются, что приводит к ошибкам в определении ε, которые могут превышать 50 %. В данной работе представлен метод, позволяющий произвести оценку параметров анизотропии непосредственно по анализу всех лучевых компонент скорости. Его суть заключается в использовании обобщенных (4-точечных) структурных функций и учете межлучевых корреляций скорости. Получено, в частности, явное выражение для поперечной структурной функции, что позволяет осуществить непосредственную проверку «закона 4/3». Апробация метода осуществлена на основе обработки данных, полученных при изучении турбулентности в конвективно-перемешанном слое покрытых льдом озер (Онежское и Вендюрское).

Ключевые слова: Акустические допплеровские профилографы течений, мелкомасштабная структура турбулентности, структурные функции, константы Колмогорова**.**

© *S. Volkov*[1], *S. Bogdanov*[1,2], *G. Zdorovennova*[1]*, *A. Terzhevik*[1], *R. Zdorovennov*[1], *N. Palshin*[1], *T. Efremova*[1], *G. Kirillin*[3]

[1]Northern Water Problems Institute, Karelian Research Centre, Russian Academy of Sciences, Petrozavodsk, Russia
[2]Petrozavodsk State University, Petrozavodsk, Russia
[3]Leibniz-Institute of Freshwater Ecology and Inland Fisheries (IGB), 12587, Müggelseedamm 310, Berlin, Germany
*E-mail: zdorovennova@gmail.com

A METHOD FOR ESTIMATION OF TURBULENCE FINE-SCALE ANISOTROPY PARAMETERS FROM ADCP DATA

Received 09.10.2020, in final form 23.12.2020

Acoustic Doppler Current Profilers (ADCP) are widely used for deriving velocity vertical profiles. In recent years these devices were also actively explored for estimations of the energy dissipation rate ε by studying longitudinal velocity structure functions (SF). However, these estimates remain questionable because the correspondent SF method is based on the assumption of the fine-scale isotropy and explores the canonical values for Kolmogorov constants. The last ones, as recent direct measurements and numerical computations prove, are highly variable, thus triggering the errors of ε estimations, which may exceed 50 %. This paper presents an approach to derive the retained information, hidden in the raw along-beam velocities data, which can shed a light on

Ссылка для цитирования: *Волков С.Ю.*, *Богданов С.Р.*, *Здоровеннова Г.Э.*, *Тержевик А.Ю.*, *Здоровеннов Р.Э.*, *Пальшин Н.И.*, *Ефремова Т.В.*, *Кириллин Г.Б.* Метод оценки параметров анизотропии мелкомасштабной турбулентности по данным акустических профилографов // Фундаментальная и прикладная гидрофизика. 2021. Т. 14, № 1. С. 86–96. doi: 10.7868/S2073667321010093

For citation: *Volkov S.*, *Bogdanov S.*, *Zdorovennova G.*, *Terzhevik A.*, *Zdorovennov R.*, *Palshin N.*, *Efremova T.*, *Kirillin G.* A Method for Estimation of Turbulence Fine-Scale Anisotropy Parameters from ADCP Data. *Fundamentalnaya i Prikladnaya Gidrofizika*. 2021, 14, 1, 86–96. doi: 10.7868/S2073667321010093

the anisotropy parameters. For this, we developed the inter-beam correlations method, based on the analysis of generalized (four-point) SF. The explicit expression for transverse SF was derived, which made it possible to check the "4/3 law" directly. The method was tested by processing velocity data, obtained from the convective mixing layer in ice-covered lakes Onega and Vendyurskoe.

Key words: Acoustic current profilers, turbulence fine-scale structure, structure functions, Kolmogorov constants.

1. Introduction

Acoustic Doppler current profilers (ADCPs) are widely used in oceanological and limnological studies. The numerous studies [1–4] had proven that under the assumption of horizontal homogeneity these devices constitute the powerful tool for mean flow vertical profiling, after the proper averaging. In recent years the progress was achieved also in processing the retained raw along-beam velocities b, including fine-scale turbulence parameters. In particular, the structure-function method SFM [5–7] and spectral inertial-dissipative method IDM [8] based on applying Taylor's hypothesis were developed for energy dissipation rate ε estimations.

Concerning the large-scale turbulence parameters, for the case of 4-beam ADCP ("Janus" configuration) the variance method was developed [9–11] and validated by estimating some components of the Reynolds stress tensor. Thus, estimates of both production and dissipation rates become available, inspiring further detailed studies of the turbulent kinetic energy balance.

On the other hand, the device applicability to turbulence studies remains restricted, and operation procedures are challenging. In particular, the problems of noise exclusion and the averaging algorithms [12, 13] still remain challenging. Another problem consists in development of appropriate data processing methods taking into account the dynamics of natural turbulent flows as well as mounting requirements for practical applications. In particular, more information on fine-scale structure and energy-containing pulsations is necessary for detailed studies of the turbulent energy balance and for estimating parameters of turbulent heat and mass transfer. The currently available ADCP operation procedures derive this information only partially. For example, in large-scale studies the above-mentioned variance method provides estimations of only two turbulence stress components; the derivation of all six components of Reynolds stress tensor is not accessible even with "Janus+" configuration of five-beam ADCP [14]. The fine-scale ADCP studies also face the problems, which, being in the focus of this paper, are discussed below in more details.

The crucial restriction of the IDM method is its inability to split along-flow and cross-flow velocity spectra. Herewith, the corresponding spectral constant remains undetermined, varying within the interval of at least (1, 4/3), even in conditions of local isotropy. As a result, the spectral fitting leads to an uncertainty for the dissipation rate estimation up to a factor of $(4/3)^{-3/2} \approx 0.65$ [8].

In turn, the performance of the SFM with regard to estimation of the energy dissipation rate ε is also sensitive to the local isotropy assumption. Namely, only longitudinal (along-beam) structural functions $D_{LL}(AA') = <(b(A') - b(A))^2>$ are available from the direct measurements of the beam velocities b at points A and A'. The corresponding estimations of ε are based on the exploring the dependence of D_{LL} on distance AA' (2/3 power law) in the inertial interval. The implementation of this procedure suggests fine-scale isotropy and, correspondingly, the use of canonical values for Kolmogorov constants. Both the validity of this assumption and, correspondently, the universality of the constants remain questionable. In different turbulence flows essential fine-scale anisotropy was revealed in numerical simulations [15], as well as experimentally [5, 7]. At that, deviations of Kolmogorov constants from their canonical ("isotropic") values may lead to the errors in dissipation rate estimations exceeding 50 %, as was proven, for instance, by direct numerical simulations of the boundary layer [16]. Such uncertainty with dissipation rate estimations are especially crucial for the problem of mixing efficiency, where the ratio of conversion of mechanical energy to background potential one is the key issue [17].

In more general context, fine-scale anisotropy and its relationship with scaling, intermittency, and spectral energy transfer remain fundamental challenges in the theory of turbulence [18]. In particular, some studies [19, 20] clearly demonstrate the necessity of distinguishing between the so-called directional (connected with different orientations of two-point separation vector) and polarization anisotropy of SF. These subtle features provide a deeper insight into the 2D-3D interplay (and corresponding k^{-3} and $k^{-5/3}$ spectra) often observed in geophysical flows [21–23].

With regard to the turbulent energy cascade and its scaling, the importance of spectra angular dependence was stressed in [24]. For stratified turbulence the exact values of scaling exponents, which identify the physical background of the energy cascade, are still challenging (e. g., Kolmogorov's 2/3 vs Bolgiano-Obukhov 6/5) [25]. Besides, a departure of high-order SF exponents from the Kolmogorov law ($2p/3$ for p-th order SF) was observed in [18], thus clearly indicating the intermittent nature of pulsations. For accurate estimations of the dissipation rate ε, the splitting up of this quantity on wave and vortex modes, as well as, horizontal and vertical parts is necessary in the general case

[26]. Most of the mentioned results and descriptors are still far above the experimental abilities. So, there are obvious gaps between recent advances in the theory of turbulence and rather restricted set of anisotropy descriptors, traditionally used by the engineering and geophysical turbulence communities.

Here, we address only the traditional Kolmogorov scaling, using the classical descriptors for anisotropy estimations: longitudinal and transverse SFs. Even this reduced version of the anisotropy problem statement is not directly applicable to ADCP measurements, because the transverse SF is not available from ADCP data. To overcome the problem, we attempted to derive the missing information from raw data, taking into account the correlation between the signals from different beams.

It should be noted that the idea to incorporate the information from all beams has been actively explored before. In particular, estimations of Reynolds stresses were successfully derived from the variances of opposite beams records for 4-beam ADCP by [9–11]. Other studies actively used the full set of data (from all beams) to improve data processing. For example, the so-called error velocity (proportional to the difference between records of pairs of opposite beams) may be used as the indicator for checking the validity of the horizontal homogeneity assumption [27]. Combining the data from all beams is often used for reducing the error of energy dissipation estimations, especially for shear flows, when the values of ε, derived from different beams data, differ significantly due to the large-scale anisotropy [5]. Here the simplest method consists of averaging the estimates obtained from different beams. A more sophisticated technique is based on the applying SF method to a composite variable similar to the error velocity [6].

It is important to note that in all mentioned examples the exploring of full (from all beams) velocity set is implemented under the assumption that the beam velocities are independent, and corresponding correlations may be neglected. The new method, presented in this paper, on the contrary, is based on taking these correlations into account. In fact, some ADCP processing in limnological [7] and marine [6] environment indirectly prove the non-zero covariance between velocity increments for different beams. In low-energetic environments, like small lakes, the revealed inertial interval has the extension of up to 1 m, commensurable with the distance between beams for rather wide depth interval. Supposedly the ADCP cross-beam correlations are not vanishing also in oceanic environment, where the scales of energy-containing structures, and, correspondently the integral scale r_c of turbulence, may exceed hundreds of meters.

The essence of the method is presented in the next section. Its technical aspects are based on studying the generalized (four-point) structure functions. The core method is designed for deeper insight into both fine- and large-scale structure of turbulence, but we concentrated first on its application to the fine-scale anisotropy. In particular, special attention is paid to the relationship between Kolmogorov constants.

2. Velocity structure function approach and turbulence isotropy

For certainty, the method is presented below for the 3-beam version of ADCP. We assume also the configuration, when the beams are equally spaced azimuthally and oriented at the angle α_0 off the vertical axis; $\alpha_0 = 25°$ in standard modifications. For such type of the device the angle $2\alpha = \angle AOB$ between the adjacent beams (fig. 1) is determined by

$$\sin\alpha = \frac{\sqrt{3}}{2}\sin\alpha_0 \approx 0.366.$$

The beam projection of the velocity is measured in a series of points along each beam, with typical cell spacing about few centimeters. For the energy dissipation rate ε in the range $10^{-9} - 10^{-6}$ W/kg, the Kolmogorov dissipative scale r_d varies from few millimeters to few centimeters. Hence, the cell spacing is usually slightly above r_d, or may be adjusted where is necessary. It means that the velocity correlations within the inertial interval in the wavelength domain (which constitute the essence of SFM) are available.

SFM for ε estimations is based on the estimation of the difference of the components of the velocity fluctuations $\vec{u}$ in some adjacent points. The matrix of the simplest (second order) SFs for two points with coordinates $\vec{x}$ and $\vec{x}+\vec{r}$ is defined as:

$$D_{ij}(\vec{x},\vec{r}) = <(\vec{u}_i(\vec{x}+\vec{r}) - \vec{u}_i(\vec{x}))(\vec{u}_j(\vec{x}+\vec{r}) - \vec{u}_j(\vec{x}))>. \quad (1)$$

The angle brackets are used for averaged (temporal mean) quantities. Hereinafter, first point with coordinates $\vec{x}$ is used as reference one.

For locally homogeneous and isotropic turbulence any element of the matrix is directly expressed through the two scalar products: the so-called longitudinal (D_{LL}) and transverse (D_{NN}) structure functions [28]:

$$D_{ij}(\vec{r}) = (D_{LL}(r) - D_{NN}(r))\frac{r_i r_j}{r^2} + D_{NN}(r)\,\delta_{ij}. \quad (2)$$

Here $r = |\vec{r}|$. Longitudinal structure function describes correlations between the components u_L of the velocity fluctuations aligned with $\vec{r}$, while D_{NN} gives the correlations of the increments of the perpendicular components.

Within the inertial interval both scalar SF obey the simple relationships

$$D_{LL}(r) = C\varepsilon^{2/3} r^{2/3}; \quad D_{NN} = \frac{4}{3} D_{LL}. \tag{3}$$

Here C is the Kolmogorov constant; for fully developed turbulence its value is close to 2.1 [16, 29]. The second equation (3) is usually treated as the "4/3 law" and usually is regarded as one of the direct criteria for checking of the local isotropy.

The raw ADCP data include only the velocity components aligned with the corresponded beams. This restriction provides, however, the ideal opportunity for longitudinal SF calculations, by choosing two points on the arbitrary beam, meaning for example points A and A' on the beam 1 (fig. 1) and calculating, with proper averaging, the beam velocity variance:

$$D_{LL} = <(b_i(A') - b_i(A))^2>. \tag{4}$$

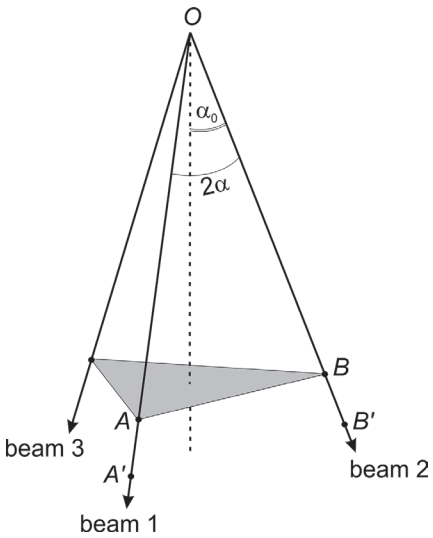

Fig. 1. Geometric configuration and key angles of 3-beams ADCP.

Here b_i (i=1, 2, 3) is the *i-th* beam velocity fluctuation at the correspondent point.

After calculating D_{LL} and taking the first equation (3) into account, the estimation of ε becomes straightforward. But this procedure works properly only under the assumption of local homogeneity and isotropy. If this assumption is violated, the value of C in (3) may deviate sufficiently from the canonical value 2.1, as direct numerical calculations prove, e.g. [15, 16].

The violation of the assumption was revealed during experimental studies in marine and limnological environments by detecting the dependence of structure functions on the direction of the vector $\vec{r}$. In particular, in most cases, the values of ε, derived after data processing from different beams, differ sufficiently [6, 7]. To provide the best estimate for ε, the values, obtained from different beams, are usually averaged, as described in Introduction. This formal smoothing procedure, ignoring the anisotropy effects, only obscures the problem and may lead to significant errors.

To obtain more reliable estimations of ε, based on SFM, the anisotropy effects must be taken into account. The ratio $a = D_{NN} / D_{LL}$ is one of the direct indicators of anisotropy, and its deviations from 4/3 may serve as the anisotropy quantitative measure. Moreover, as shown in [15, 16], the parameter a strongly correlates with the values of Kolmogorov constants. However, the methods of D_{NN} estimations are underdeveloped. To overcome the problem, the generalized (four-point) structure functions may be involved, as presented in the next section.

3. Inter-beam velocity structure function: definition, derivation, and interpretation

The missing information on the fine-scale anisotropy may be potentially derived from inter-beam correlations. For this, generalized (four-point) structural functions $\tilde{D}$ may be introduced, which describe the correlations between velocity increments for two pairs of points on different beams. For example, two pairs (A, A') and (B, B') on the beams 1 and 2 (fig. 1) yield:

$$\tilde{D}_{12} = <(b_{A'1} - b_{A1})(b_{B'2} - b_{B2})>. \tag{5}$$

To avoid bulky calculations and to present the method idea more clearly, we chose the simplest geometrical configuration: points A and B are located at the same depth and $AA' = BB'$. The expressions derived below are easily extended on the general case.

The values of $\tilde{D}_{12}$ for different distances $l = AB$ and $r = AA'$ are easily derived from experimental data, because beam velocities at all chosen points are measured directly. On the other hand, assuming local isotropy, these values are readily represented [28] through the values of ordinary structure functions with properly chosen arguments (the detailed calculations are moved to the Appendix):

$$2\tilde{D}_{12} = (\cos 2\alpha - \cos 2\beta) D_{LL}(A'B) + \frac{1}{2}(1 - \cos 2\alpha)(D_{LL}(AB) + D_{LL}(A'B')) +$$
$$+ (\cos 2\alpha + \cos 2\beta) D_{NN}(A'B) - \frac{1}{2}(1 + \cos 2\alpha)(D_{NN}(AB) + D_{NN}(A'B')). \tag{6}$$

Here, α is determined by the device-dependent beam angle α_0, as presented above; the value of the angle $\beta = \angle ABA'$ is determined from the equation $\sin\beta = (r/l)\cos(\alpha+\beta)$ (see Appendix).

Formula (6) links the values D_{NN} with $\tilde{D}_{12}$ and D_{LL}, the latter two directly available from experimental data. There are several ways for further application of Eq. (6) in anisotropy studies. First, one can treat this formula as the explicit expression, binding the values of transverse structural function with three different values of argument. In any case, this expression may be helpful for the direct D_{NN} estimations. Second, assuming local isotropy relation $D_{NN} = \frac{4}{3} D_{LL}$ one can rewrite (7) as an alternative representation for longitudinal SF from Eq. (3):

$$12\tilde{D}_{12} = 2(7\cos 2\alpha + \cos 2\beta) D_{LL}(A'B) - (1 + 7\cos 2\alpha)(D_{LL}(AB) + D_{LL}(A'B')). \quad (7)$$

Formula (7) gives the opportunity to check the local isotropy by negative proof method. The third implementation is similar to the previous, but looks more illustrative. Introducing parameter $a \equiv D_{NN} / D_{LL}$ for SF ratio (instead of prescribed 4/3), equation (7) is transformed to:

$$\begin{aligned} 2\tilde{D}_{12} = ((1+a)\cos 2\alpha - (1-a)\cos 2\beta) D_{LL}(A'B) + \\ + ((1-a) - (1+a)\cos 2\alpha)(D_{LL}(AB) + D_{LL}(A'B')) / 2, \end{aligned} \quad (8)$$

which makes it possible to calculate parameter a directly. Below we use (8) as the basic formula for checking the local isotropy, by comparing calculated value of the parameter a with the canonical value 4/3.

Implementation of Eq. (8) is not straightforward, because the right hand side of (8) includes the values of D_{LL} for three different arguments (AB, $A'B$, $A'B'$) and two reference points (A and A'), increasing by this the noise level. Minimizing of the negative effect is possible by specific choice of the relative point orientation. For example, we may choose the point A' in such a way, that $A'B = A'B'$. For this special configuration $\beta = 2\alpha$, $A'B' = \frac{l}{2\cos 2\alpha - 1}$ (see Appendix). As a result, Eq. (8) is reduced to:

$$\begin{aligned} 2\tilde{D}_{12} = ((1-a)/2 + (1+a)(\cos 2\alpha)/2 - (1-a)\cos 4\alpha) D_{LL}(A'B') + \\ + ((1-a) - (1+a)\cos 2\alpha) D_{LL}(AB)/2. \end{aligned} \quad (9)$$

Eq. (9) includes the values of D_{LL} only for two arguments (AB and $A'B'$). The expression for a follows from (9) in a straight way:

$$a = \frac{4\tilde{D}_{12} - (\cos 2\alpha - 2\cos 4\alpha + 1) D_{LL}(A'B') - (1 - \cos 2\alpha) D_{LL}(AB)}{(\cos 2\alpha + 2\cos 4\alpha - 1) D_{LL}(A'B') - (1 + \cos 2\alpha) D_{LL}(AB)}. \quad (10)$$

Numerator and denominator on the right side of (10) are presented by linear combinations of longitudinal structure functions with arguments AB and $A'B'$. The corresponding coefficients depend only on angle α, whose value is, in turn, prescribed by the device beam angle α_0.

The explicit relation (10) for the parameter a makes it possible to verify the "4/3 law", which is traditionally viewed as the main necessary criterion for the local isotropy hypothesis applicability.

4. Application to field observations

We applied the abovementioned method, based on the inter-beams velocity correlations, to derive some additional information on turbulence structure of the convectively mixed layer, which develops in ice-covered lakes in spring as a result of inhomogeneous heating of water by solar radiation [3, 30].

The field experiments were carried out during the spring convection in the central deep-water part of Lake Vendyurskoe, Russia at 8–13 April 2016 and in Petrozavodsk Bay of Onega Lake at 12–20 March 2017. The 2 MHz HR Aquadopp Nortek profiler in the pulse-to-pulse coherent mode scanned roughly 2-m thick layer with the blind zone of the first 15 cm from the device head. The details of experimental setup are presented in [7, 23].

For both lakes we calculated D_{LL} by averaging of the beam velocity increments for each beam and revealed the inertial interval which covered at least one decade of scales and extended up to the value $L_i \sim$ (0.5–0.7) m (fig. 2, see Inset). Due to the latter finding, the value of turbulence integral scale should be expected as 1 m and more. Herewith, the signals from points on different beams, separated by the distance less than ~1 m, cannot be regarded independent. Hence, the inter-beams velocity covariance is not vanishing, offering the opportunity to estimate the local anisotropy by the described method.

Taking this into account, we focused on estimation the parameter a. For this we used the expression (10), which corresponds to the reduced version of points configuration ($A'B = A'B'$ and $\beta = 2\alpha$).

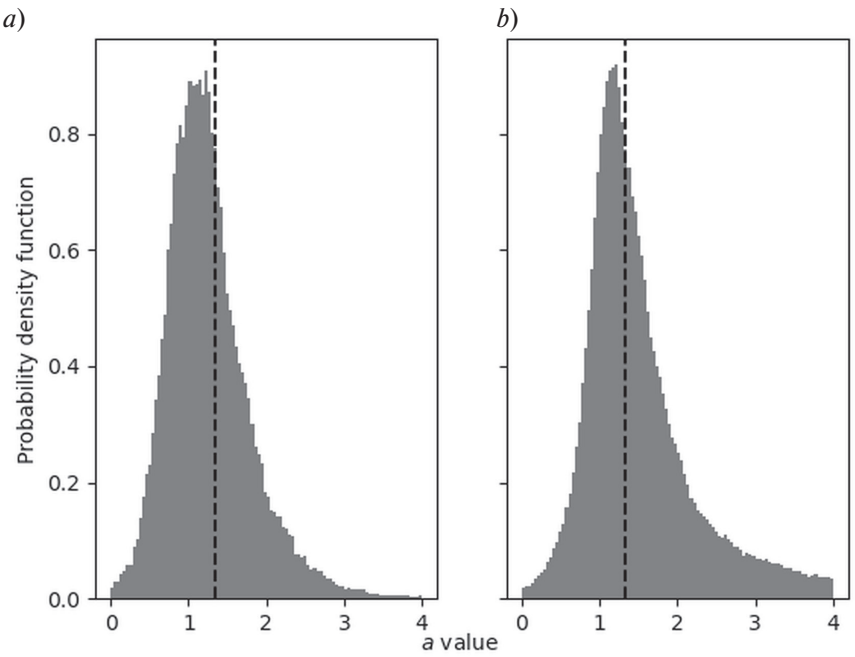

Fig. 3. Probability density function for anisotropy parameter a. *a* — Lake Vendyurskoe, *b* — Onega Lake. Dashed lines correspond to the classical value 4/3 of the parameter a.

Data processing included several preliminary steps. First, data was cleaned by simple filter dropping out the records deviating from the average burst velocity by the value exceeding 2.5 σ (here σ is standard deviation). Then each burst was averaged to get evenly time indexed dataset. To complete the preprocessing, the beam velocity fluctuations were calculated by subtraction of the 30-min moving average.

The proper choice of the reference points and the corresponding range of appropriate values of OA (along beam distance between ADCP and one of the upper reference points), is the most important feature for the method implementation. Here we followed the criteria $A'B' < L_i$. Taking into account the formulas, which connect the values of segments $A'B'$ and AB, AB and OA (see Appendix), the arguments of D_{LL} in (10) are expressed directly through the distance OA (along beam distance between ADCP and one of the upper reference points): $A'B' \approx 2.15\ AB$; $AB \approx 0.73\ OA$. At the same time, these estimates give the upper limit for OA: $OA \approx 0.64\ A'B' < 0.64\ L_i$.

Fig. 3 presents the calculated values of a for the entire period of measurements and for all available along-beam distances OA, for both lakes. These values were averaged over all three pairs of beams; the negative values, as well as the values exceeding 3, were dropped. The calculations demonstrate the high level of the parameter a variations with time and depth. The histograms additionally illustrate that distribution of a is skewed. For both lakes the mean values of a exceed the canonical value 4/3: $a = 1.77 \pm 0.59$ and $a = 1.38 \pm 0.35$ for Onega Lake and Lake Vendyurskoe, respectively. This result is consistent with DNS findings, derived for boundary layer [16].

5. Discussion

Data processing from inter-beam correlations includes some subtle features. It should be stressed that implementation of the proposed method is crucially sensitive to the choice of ADCP settings. The cell size S and the extent L of the scanned area must be properly adjusted for each specific case. The value of S should be rather small for reliable estimations of SF and large enough compared with the dissipative scale r_d. On the other hand, the method works, when the signals within the whole scanned area are correlated. Therefore, the length L should be chosen by taking into account the integral scale of turbulence or, more correctly, the extent L_i of the inertial interval. In particular, the simple criteria $L \le L_i$ appears appropriate.

Another specific issue concerns the structure of the derived calculation formulas. For example, both (6) and (10) one can treat as the expressions, which directly connect the anisotropy descriptors (D_{NN} and a correspondently) and the standard longitudinal SF. However, to estimate these descriptors, the values of D_{LL} are necessary for different values of argument and, more important, for different reference points. This feature increases the error level, so that processing of noisy data becomes more sophisticated and imposes some limitations on the method's scope of application. The problem of reducing the error level remains most challenging for the method application and is addressed for the future studies.

Besides, the multiplicity of reference points in formulas involves additional restrictions: the slow spatial variations of the energy dissipation rate ε (and, correspondently, D_{LL}) must be taken into account for general (inhomogeneous) case, leading to the problem of splitting the anisotropy and inhomogeneity effects. In order to avoid the last problem, we tested the method by its application to the case of radiatively-driven convection, when convectively mixed layer is usually regarded as vertically homogeneous, and variations of ε within this layer are relatively small [30].

In this study, the inter-beam correlation method was established and applied to the analysis of fine-scale anisotropy parameters. However, the scope of the method can be extended beyond these issues. In particular, the relationship between the generalized and ordinary structural functions may also be used to derive missing expressions for Reynolds stress components, after proper choice of the pairs of points. Namely, the expression (6) gives the explicit presentation for the corresponding stress for the case of reduced set of four points, with two of them coinciding. For example, the set of pairs (*A*, *E*) and (*E*, *B*) (fig. 4) is sufficient for calculating the Reynolds stress component $<b_1 b_2>$. By this, the method provides the opportunity to study the fine- and large-scale anisotropy independently gaining a new insight into the problem of identifying the presumable "fingerprints" of energy-containing structures at smaller scales [16, 20, 31].

6. Conclusions

The advanced SF method, based on the use of the four-point correlation functions, gives the broader opportunities in analyzing the turbulence fine–scale structure by processing the ADCP data. In particular the inter-beam correlation method, established in this paper, makes it possible to derive the explicit expressions, which connect the values of longitudinal and transverse SF with directly measured quantities. These expressions were used for checking the local isotropy assumption, and, in particular, the validity of the famous relationship $D_{NN} = (4/3)\, D_{LL}$. The data analysis revealed the significant spatial and time variability of the constant *a*. At that for both lakes its values exceed the canonical value 4/3. So, the estimations of the energy dissipation rate, derived from longitudinal SF, in most cases need to be corrected.

7. Funding

The study was carried out under state order to the Northern water problems Institute of Karelian Research Center of RAS. GK was supported by the German Research Foundation (DFG Projects KI 853–13/1 and KI 853–16/1) and by the Sino-German Center for Research Support (CDZ Project GZ 1259).

Appendix. Representation for generalized structure function

To derive the relationship between the generalized structure function $\tilde{D}_{12}$ and the ordinary ones, we consider the plane, which include any two of three beams (for example, beam 1 and beam 2 on fig. 4). The orthogonal axes *X* and *Y* are introduced as presented by fig. 4.

The distances *AA′*, *AB* and the depth *OE* of the reference points *A*, *B* are denoted as *r*, *l* and h_0, respectively. Then, the depth difference *h*, the lengths of segments *A′B* and *A′B′*, and the depth h_0 are determined by the simple expressions:

$$h = r\cos\alpha; \quad A'B' = l + 2r\sin\alpha;$$

$$A'B = l\frac{\cos\alpha}{\cos(\alpha+\beta)}; \; h_0 = (l\, ctg\alpha)/2.$$

We also put into consideration the angle $\beta \equiv \angle ABA'$; the expression for this angle is derived directly by applying the sinus theorem:

$$\sin\beta = (r/l)\cos(\alpha+\beta)..$$

For special configuration of points, when $A'B = A'B'$ and $\beta = 2\alpha$, the expression for the lengths of both segments is reduced to $A'B' = \dfrac{l}{2\cos 2\alpha - 1}$.

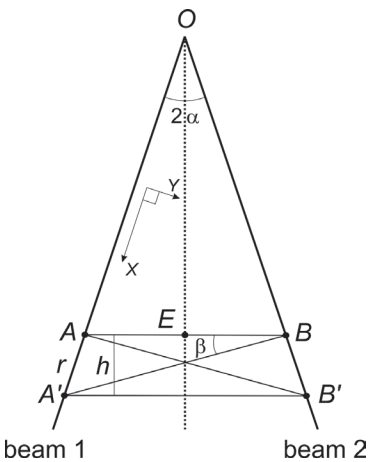

Fig. 4. Four-point configuration for generalized structure function.

In the *XY* frame of reference the beam velocities are expressed as linear combinations of velocity components at the correspondent points: $b_1(A) = u_X(A)$; $b_2(B) = u_X(B)\cos 2\alpha + u_Y(B)\sin 2\alpha$, and similar expressions for points *A′* and *B′*. Substituting these expressions into formula (6), we derive:

$$\tilde{D}_{12} = \tilde{D}_{XX}\cos 2\alpha + \tilde{D}_{XY}\sin 2\alpha.$$

Here, both terms at right-hand side are presented by correlations of the increments of Cartesian components at two different pairs of points:

$$\tilde{D}_{XX} = <(u_X(A') - u_X(A))(u_X(B') - u_X(B))>,$$
$$\tilde{D}_{XY} = <(u_X(A') - u_X(A))(u_Y(B') - u_Y(B))>.$$

Both correlations are not available from the experiment, because at each point only beam component of the velocity, rather than both Cartesian projections, are measured directly.

On the other hand, both generalized four-point functions $\tilde{D}_{XX}$ and $\tilde{D}_{XY}$ may be expressed through the ordinary SF by the following conversion formula [28]:

$$\tilde{D}_{XX} = \frac{1}{2}(D_{XX}(\overrightarrow{A'B}) + D_{XX}(\overrightarrow{AB'}) - D_{XX}(\overrightarrow{A'B'}) - D_{XX}(\overrightarrow{AB})). \quad \text{(A1)}$$

The similar expression is valid for the function $\tilde{D}_{XY}$.

Each term on the right hand side of the last equation may be expressed through the longitudinal and transverse SF in a standard way, by using formula (5) and substituting

$$\overrightarrow{A'B},\ \overrightarrow{AB'},\ \overrightarrow{A'B'} \text{ and } \overrightarrow{AB} \text{ as } \vec{r} \text{ in series.}$$

The corresponding unit vectors are calculated directly:

$$(-\sin(\alpha+\beta), \cos(\alpha+\beta)) \text{ — for } \overrightarrow{A'B}$$
$$(-\sin(\alpha-\beta), \cos(\alpha-\beta)) \text{ — for } \overrightarrow{AB'}$$
$$(-\sin\alpha, \cos\alpha) \text{ — for } \overrightarrow{AB} \text{ and } \overrightarrow{A'B'}.$$

By taking into account these expressions for the direction cosines, for the terms in the right-hand side in formula (A1) the following representations are easily derived:

$$D_{XX}(\overrightarrow{AB}) = (D_{LL}(AB) - D_{NN}(AB))\sin^2\alpha + D_{NN}(AB);$$
$$D_{XX}(\overrightarrow{A'B}) = (D_{LL}(A'B) - D_{NN}(A'B))\sin^2(\alpha+\beta) + D_{NN}(A'B);$$
$$D_{XX}(\overrightarrow{AB'}) = (D_{LL}(AB') - D_{NN}(AB'))\sin^2(\alpha-\beta) + D_{NN}(AB').$$

The expression for $D_{XX}(\overrightarrow{A'B'})$ is the same as for $D_{XX}(\overrightarrow{AB})$: only substituting AB by $A'B'$ is necessary.

The last set of formulas establishes the linear relationships between $\tilde{D}_{XX}$ and D_{LL}, D_{NN}, with simple trigonometric coefficients. The similar is true for $\tilde{D}_{XY}$.

Finally, the expression for $\tilde{D}_{12}$ takes the form:

$$2\tilde{D}_{12} = c_1 D_{LL}(A'B) + c_2(D_{LL}(AB) + D_{LL}(A'B')) + \\ + c_3 D_{NN}(A'B) - c_4(D_{NN}(AB) + D_{NN}(A'B')). \quad \text{(A2)}$$

Here c_i — trigonometric factors, defined by the relations:

$$c_1 = \cos 2\alpha - \cos 2\beta;\ c_2 = (1-\cos 2\alpha)/2;\ c_3 = \cos 2\alpha + \cos 2\beta;\ c_4 = (1+\cos 2\alpha)/2.$$

When point A is close to B, and A' — to B', and, correspondingly, $\alpha \to 0;\ \beta \to \pi/2,$ the factors take the values 2, 0, 0, 1 and formula (A2) is reduced to $\tilde{D}_{12} = D_{LL},$ as expected.

The last equation for $\tilde{D}_{12}$ is similar to formula (6) presented in the main text.

Литература

1. *Greene A.D.*, *Hendricks P.J.*, *Gregg M.C.* Using an ADCP to estimate turbulent kinetic energy dissipation rate in sheltered coastal waters // J. Atmos. Oceanic Technol. 2015. V. 32, N 2. P. 318–333. doi: 10.1175/JTECH-D-13–00207.1
2. *Kirillin G.B.*, *Forrest A.L.*, *Graves K.E.*, *Fischer A.*, *Engelhardt C.*, *Laval B.E.* Axisymmetric circulation driven by marginal heating in ice-covered lakes // Geophys. Res. Lett. 2015. V. 42, N 8. P. 2893–2900. doi: 10.1002/2014GL062180
3. *Bouffard D.*, *Wüest A.* Convection in lakes // Annu. Rev. Fluid Mech. 2019. V. 51. P. 189–215. doi: 10.1146/annurev-fluid-010518–040506
4. *Flood B.*, *Wells M.*, *Dunlop E.*, *Young J.* Internal waves pump waters in and out of a deep coastal embayment of a large lake // Limnol. Oceanogr. 2020. V. 65, N 2. P. 205–223. doi: 10.1002/lno.11292
5. *Wiles P.J.*, *Rippeth T.P.*, *Simpson J.H.*, *Hendricks P.J.* A novel technique for measuring the rate of turbulent dissipation in the marine environment // Geophys. Res. Lett. 2006. V. 33, N 21. L21608. doi: 10.1029/2006GL027050
6. *Lucas N.S.*, *Simpson J.H.*, *Rippeth T.P.*, *Old C.P.* Measuring Turbulent Dissipation Using a Tethered ADCP // J. Atmos. Oceanic Technol. 2014. V. 31. P. 1826–1837. doi: 10.1175/JTECH-D-13–00198.1

7. *Volkov S.*, *Bogdanov S.*, *Zdorovennov R.*, *Zdorovennova G.*, *Terzhevik A.*, *Palshin N.*, *Bouffard D.*, *Kirillin G.* Fine scale structure of convective mixed layer in ice-covered lake // Environ. Fluid Mech. 2019. V. 19. P. 751–764. doi: 10.1007/s10652–018–9652–2
8. *Lorke A.*, *Wüest A.* Application of Coherent ADCP for Turbulence Measurements in the Bottom Boundary Layer // J. Atmos. Oceanic Technol. 2005. V. 22. P. 1821–1828. doi: 10.1175/JTECH1813.1
9. *Howarth M.J.*, *Souza A.J.* Reynolds stress observations in continental shelf seas // Deep Sea Res II. 2005. V. 52, N 9. P. 1075–1086. doi: 10.1016/j.dsr2.2005.01.003
10. *Whipple A.C.*, *Luettich R.A. Jr.*, *Seim H.E.* Measurements of Reynolds stress in a wind-driven lagoonal estuary // Ocean Dyn. 2006. V. 56. P. 169–185. doi: 10.1007/s10236–005–0038-x
11. *Rosman J.H.*, *Hench J.L.*, *Koseff J.R.*, *Monismith S.G.* Extracting Reynolds Stresses from Acoustic Doppler Current Profiler Measurements in Wave-Dominated Environments // J. Atmos. Oceanic Technol. 2008. V. 25. P. 286–306. doi: 10.1175/2007JTECHO525.1
12. *Whipple A.C.*, *Luettich R.A.* A comparison of acoustic turbulence profiling techniques in the presence of waves // Ocean Dyn. 2009. V. 59. P. 719. doi: 10.1007/s10236–009–0208–3
13. *Kirincich A.R.*, *Rosman J.H.* A Comparison of Methods for Estimating Reynolds Stress from ADCP Measurements in Wavy Environments // J. Atmos. Oceanic Technol. 2011. V. 28. P. 1539–1553. doi: 10.1007/s10236–009–0208–3
14. *Guerra M.*, *Thomson J.* Turbulence Measurements from Five-Beam Acoustic Doppler Current Profilers // J. Atmos. Oceanic Technol. 2017. V. 34. P. 1267–1284. doi: 10.1175/JTECH-D-16–0148.1
15. *Jabbari A.*, *Boegman L.*, *Piomelli U.* Evaluation of the inertial dissipation method within boundary layers using numerical simulations // Geophys. Res. Lett. 2015. V. 42, N 5. P. 1504–1511. doi: 10.1002/2015GL063147
16. *Jabbari A.*, *Rouhi A.*, *Boegman L.* Evaluation of the structure function method to compute turbulent dissipation within boundary layers using numerical simulations // J. Geophys. Res. Oceans. 2016. V. 121, N 8. doi: 10.1002/2015JC011608
17. *Peltier W.R.*, *Caulfield C.P.* Mixing efficiency in stratified shear flows // Annu. Rev. Fluid Mech. 2003. V. 35. P. 135–167. doi: 10.1146/annurev.fluid.35.101101.161144
18. *Biferale L.* Shell models of energy cascade in turbulence // Annu. Rev. Fluid Mech. 2003. V. 35. P. 441–468. doi: 10.1146/annurev.fluid.35.101101.161122
19. *Kassinos S.*, *Reynolds W.*, *Rogers M.* One-point turbulence structure tensors // J. Fluid Mech. 2001. V. 428. P. 213–248. doi: 10.1017/S0022112000002615
20. *Cambon C.* Strongly Anisotropic Turbulence, Statistical Theory and DNS / Eds. Deville M., Lê TH., Sagaut P. Turbulence and Interactions. Notes on Numerical Fluid Mechanics and Multidisciplinary Design, v. 105. Berlin, Heidelberg: Springer, 2009. doi: 10.1007/978–3–642–00262–5_1
21. *Lilly D.K.* Stratified turbulence and the mesoscale variability of the atmosphere // J. Atmos. Sci. 1983. V. 40. P. 749–761. doi: 10.1175/1520–0469(1983)040<0749: STATMV>2.0.CO;2
22. *Lindborg E.* The energy cascade in a strongly stratified fluid // J. Fluid. Mech. 2006. V. 550. P. 207–242. doi: 10.1017/S0022112005008128
23. *Bogdanov S.*, *Zdorovennova G.*, *Volkov S.*, *Zdorovennov R.*, *Palshin N.*, *Efremova T.*, *Terzhevik A.*, *Bouffard D.* Structure and dynamics of convective mixing in Lake Onego under ice-covered conditions // Inland Waters. 2019. V. 9, N 2. P. 177–192. doi: 10.1080/20442041.2018.1551655
24. *Casciola C.M.*, *Gualtieri P.*, *Jacob B.*, *Piva R.* Scaling Properties in the Production Range of Shear Dominated Flows // Phys. Rev. Lett. 2005. V. 95. 024503. doi: 10.1103/PhysRevLett.95.024503
25. *Lohse D.*, *Xia K.-Q.* Small-Scale Properties of Turbulent Rayleigh-Bénard Convection // Annu. Rev. Fluid Mech. 2010. V. 42. P. 335–364. doi: 10.1146/annurev.fluid.010908.165152
26. *Kimura Y.*, *Herring J.R.* Energy spectra of stably stratified turbulence // J. Fluid. Mech. 2012. V. 698. P. 19–50. doi: 10.1017/jfm.2011.546
27. *Gilcoto M.*, *Jones E.*, *Fariña-Busto L.* Robust Estimations of Current Velocities with Four-Beam Broadband ADCPs // J. Atmos. Oceanic Technol. 2009. V. 26, N 12. P. 2642–2654.
28. *Monin A.S.*, *Yaglom A.M.* Statistical fluid mechanics. Cambridge, Mass.: M.I.T. Press, 1971.
29. *Chandrasekhar S.* The theory of axisymmetric turbulence // Philosophical Transactions of the Royal Society of London. Series A, Mathematical and Physical Sciences. 1950. V. 242. P. 557–577. doi: 10.1098/rsta.1950.0010
30. *Jonas T.*, *Terzhevik A.Y.*, *Mironov D.V.*, *Wüest A.* Radiatively driven convection in an ice-covered lake investigated by using temperature microstructure technique // J. Geophys. Res. 2003. V. 108, N C6. 3183. doi: 10.1029/2002JC001316
31. *Bogdanov S.R.* Kolmogorov constants in the spectra of anisotropic turbulence // J. Appl. Mech. Tech. Phys. 1990. V. 31, 802. doi: 10.1007/BF00852459

References

1. *Greene A.D.*, *Hendricks P.J.*, *Gregg M.C.* Using an ADCP to Estimate Turbulent Kinetic Energy Dissipation Rate in Sheltered Coastal Waters. *J. Atmos. Oceanic Technol.* 2015, 32(2), 318–333. doi: 10.1175/JTECH-D-13–00207.1

2. *Kirillin G.B.*, *Forrest A.L.*, *Graves K.E.*, *Fischer A.*, *Engelhardt C.*, *Laval B.E.* Axisymmetric circulation driven by marginal heating in ice-covered lakes. *Geophys. Res. Lett.* 2015, 42(8), 2893–2900. doi: 10.1002/2014GL062180
3. *Bouffard D.*, *Wüest A.* Convection in lakes. *Annu. Rev. Fluid Mech.* 2019, 51, 189–215. doi: 10.1146/annurev-fluid-010518–040506
4. *Flood B.*, *Wells M.*, *Dunlop E.*, *Young J.* Internal waves pump waters in and out of a deep coastal embayment of a large lake. *Limnol. Oceanogr.* 2020, 65(2), 205–223. doi: 10.1002/lno.11292
5. *Wiles P.J.*, *Rippeth T.P.*, *Simpson J.H.*, *Hendricks P.J.* A novel technique for measuring the rate of turbulent dissipation in the marine environment. *Geophys. Res. Lett.* 2006, 33(21), L21608. doi: 10.1029/2006GL027050
6. *Lucas N.S.*, *Simpson J.H.*, *Rippeth T.P.*, *Old C.P.* Measuring Turbulent Dissipation Using a Tethered ADCP. *J. Atmos. Oceanic Technol.* 2014, 31, 1826–1837. doi: 10.1175/JTECH-D-13–00198.1
7. *Volkov S.*, *Bogdanov S.*, *Zdorovennov R.*, *Zdorovennova G.*, *Terzhevik A.*, *Palshin N.*, *Bouffard D.*, *Kirillin G.* Fine scale structure of convective mixed layer in ice-covered lake. *Environ. Fluid Mech.* 2019, 19, 751–764. doi: 10.1007/s10652–018–9652–2
8. *Lorke A.*, *Wüest A.* Application of coherent ADCP for turbulence measurements in the bottom boundary layer. *J. Atmos. Oceanic Technol.* 2005, 22, 1821–1828. doi: 10.1175/JTECH1813.1
9. *Howarth M.J.*, *Souza A.J.* Reynolds stress observations in continental shelf seas. *Deep Sea Res II.* 2005, 52, 9, 1075–1086. doi: 10.1016/j.dsr2.2005.01.003
10. *Whipple A.C.*, *Luettich R.A. Jr.*, *Seim H.E.* Measurements of Reynolds stress in a wind-driven lagoonal estuary. *Ocean Dyn.* 2006, 56, 169–185. doi: 10.1007/s10236–005–0038-x
11. *Rosman J.H.*, *Hench J.L.*, *Koseff J.R.*, *Monismith S.G.* Extracting Reynolds Stresses from Acoustic Doppler Current Profiler Measurements in Wave-Dominated Environments. *J. Atmos. Oceanic Technol.* 2008, 25, 286–306. doi: 10.1175/2007JTECHO525.1
12. *Whipple A.C.*, *Luettich R.A.* A comparison of acoustic turbulence profiling techniques in the presence of waves. *Ocean Dynamics*. 2009, 59, 719. doi: 10.1007/s10236–009–0208–3 13. *Kirincich A.R.*, *Rosman J.H.* A Comparison of Methods for Estimating Reynolds Stress from ADCP Measurements in Wavy Environments. *J. Atmos. Oceanic Technol.* 2011, 28, 1539–1553. doi: 10.1007/s10236–009–0208–3
14. *Guerra M.*, *Thomson J.* Turbulence measurements from five-beam acoustic doppler current profilers. *J. Atmos. Oceanic Technol.* 2017, 34, 1267–1284. doi: 10.1175/JTECH-D-16–0148.1
15. *Jabbari A.*, *Boegman L.*, *Piomelli U.* Evaluation of the inertial dissipation method within boundary layers using numerical simulations. *Geophys. Res. Lett.* 2015, 42, 5, 1504–1511. doi: 10.1002/2015GL063147
16. *Jabbari A.*, *Rouhi A.*, *Boegman L.* Evaluation of the structure function method to compute turbulent dissipation within boundary layers using numerical simulations. *J. Geophys. Res. Oceans.* 2016, 121, 8. doi: 10.1002/2015JC011608
17. *Peltier W.R.*, *Caulfield C.P.* Mixing efficiency in stratified shear flows. *Annu. Rev. Fluid Mech.* 2003, 35 (1), 135–167. doi: 10.1146/annurev.fluid.35.101101.161144
18. *Biferale L.* Shell models of energy cascade in turbulence. *Annu. Rev. Fluid Mech.* 2003, 35(1), 441–468. doi: 10.1146/annurev.fluid.35.101101.161122
19. *Kassinos S.*, *Reynolds W.*, *Rogers M.* One-point turbulence structure tensors. *J. Fluid Mech.* 2001, 428, 213–248. doi: 10.1017/S0022112000002615
20. *Cambon C.* Strongly Anisotropic Turbulence, Statistical Theory and DNS. *Turbulence and Interactions. Notes on Numerical Fluid Mechanics and Multidisciplinary Design*. Eds. Deville M., Lê TH., Sagaut P. *Springer*, *Berlin*, *Heidelberg*. 2009, 105. doi: 10.1007/978–3–642–00262–5_1
21. *Lilly D.K.* Stratified turbulence and the mesoscale variability of the atmosphere. *J. Atmos. Sci.* 1983, 40, 749–761. doi: 10.1175/1520–0469(1983)040<0749: STATMV>2.0.CO;2
22. *Lindborg E.* The energy cascade in a strongly stratified fluid. *J. Fluid. Mech.* 2006, 550, 207–242. doi: 10.1017/S0022112005008128
23. *Bogdanov S.*, *Zdorovennova G.*, *Volkov S.*, *Zdorovennov R.*, *Palshin N.*, *Efremova T.*, *Terzhevik A.*, *Bouffard D.* Structure and dynamics of convective mixing in Lake Onego under ice-covered conditions. *Inland Waters*. 2019, 9(2), 177–192. doi: 10.1080/20442041.2018.1551655
24. *Casciola C.M.*, *Gualtieri P.*, *Jacob B.*, *Piva R.* Scaling Properties in the Production Range of Shear Dominated Flows. *Phys. Rev. Lett.* 2005, 95, 024503. doi: 10.1103/PhysRevLett.95.024503
25. *Lohse D.*, *Xia K.-Q.* Small-Scale Properties of Turbulent Rayleigh-Bénard Convection. *Annu. Rev. Fluid Mech.* 2010, 42, 1, 335–364. doi: 10.1146/annurev.fluid.010908.165152
26. *Kimura Y.*, *Herring J.R.* Energy spectra of stably stratified turbulence. *J. Fluid. Mech.* 2012, 698, 19–50. doi:10.1017/jfm.2011.546
27. *Gilcoto M.*, *Jones E.*, *Fariña-Busto L.* Robust Estimations of Current Velocities with Four-Beam Broadband ADCPs. *J. Atmos. Oceanic Technol.* 2009, 26, 2642–2654.

28. *Monin A.S.*, *Yaglom A.M.* Statistical fluid mechanics, M.I.T. Press, Cambridge, Mass., 1971.
29. *Chandrasekhar S.* The theory of axisymmetric turbulence. *Philosophical Transactions of the Royal Society of London. Series A*, *Mathematical and Physical Sciences*. 1950, 242, 557–577. doi: 10.1098/rsta.1950.0010
30. *Jonas T.*, *Terzhevik A.Y.*, *Mironov D.V.*, *Wüest A.* Radiatively driven convection in an ice-covered lake investigated by using temperature microstructure technique. *J. Geophys. Res.* 2003, 108, C6, 3183. doi: 10.1029/2002JC001316
31. *Bogdanov S.R.* Kolmogorov constants in the spectra of anisotropic turbulence. *J. Appl. Mech. Tech. Phys*. 1990, 31, 802. doi: 10.1007/BF00852459

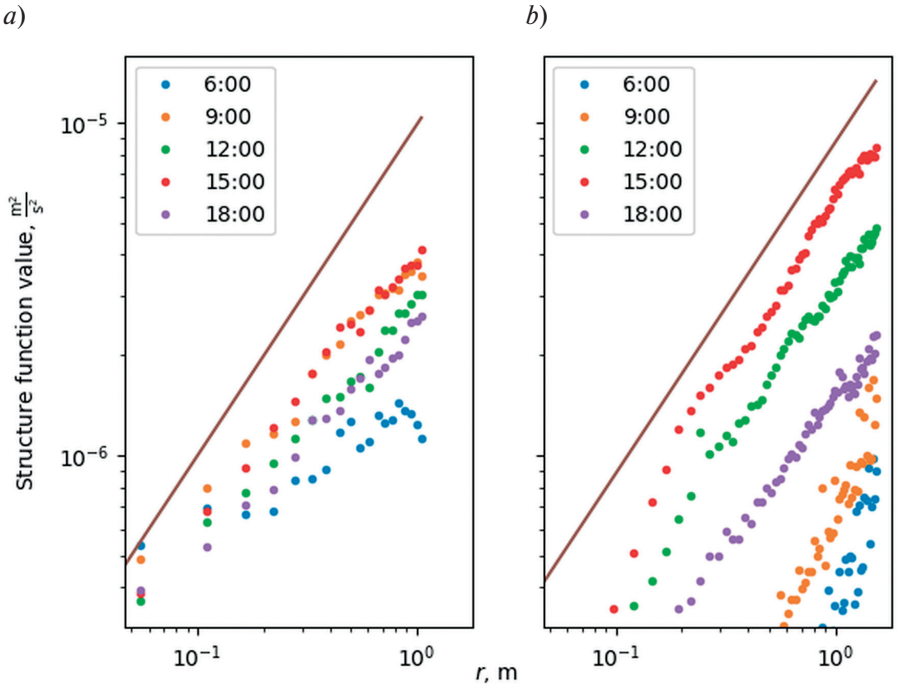

Fig. 2. The series of longitudinal velocity structure functions in the spatial domain: *a* — Lake Vendyurskoe, 10 April 2016, *b* — Lake Onega, 15 March 2017. Bold lines correspond to $r^{2/3}$ slope.